EBioMedicine 60 (2020) 102996

Contents lists available at ScienceDirect

EBioMedicine

journal homepage: www.elsevier.com/locate/ebiom

A novel HER2-targeting antibody 5G9 identified by large-scale trastuzumab-based screening exhibits potent synergistic antitumor activity

Xiaoyu Ding[a,b,1], Wanjian Gu[c,1], Yujie Zhong[a,b,1], Xiaoyao Hao[d], Jinyu Liu[d], Shukai Xia[d], Lan Luo[b,*], Mingjiu Chen[d,*], Chunni Zhang[a,b,**]

[a] Department of Clinical Laboratory, Jinling Hospital, State Key Laboratory of Analytical Chemistry for Life Science, School of Life Sciences, Nanjing University, Nanjing, Jiangsu, China
[b] State Key Laboratory of Pharmaceutical Biotechnology, School of Life Sciences, Nanjing University, Nanjing, Jiangsu, China
[c] Department of Clinical Laboratory, Affiliated Hospital of Nanjing University of Chinese Medicine, Nanjing, Jiangsu, China
[d] Biosion Inc., Nanjing, Jiangsu, China

ARTICLE INFO

Article History:
Received 13 March 2020
Revised 24 August 2020
Accepted 25 August 2020
Available online xxx

Keywords:
Large-scale screening
5G9
Trastuzumab
Pertuzumab
Synergistic efficacy

ABSTRACT

Background: Pertuzumab is currently used in combination with trastuzumab as the first-line treatment for HER2-positive metastatic breast cancer. However, pertuzumab was originally developed independently from trastuzumab and was later incidentally found to have synergistic efficacy when combined with trastuzumab, it remains to be seen whether a more potent synergistic efficacy partner exists for trastuzumab.
Methods: A trastuzumab-based functional assay was used to screen anti-HER2 antibodies harboring trastuzumab-synergistic antitumor activity. The lead candidate 5G9, in combination with trastuzumab, was further characterized for its bioactivities in cell proliferation, cell apoptosis, antigen-antibody endocytosis and HER2-mediated cell signaling pathway blocking. Finally, animal models were used to evaluate the *in vivo* synergistic antitumor efficacy of 5G9 in combination with trastuzumab.
Findings: Compared to pertuzumab, 5G9 demonstrated more potent synergistic cell growth inhibitory activity when combined with trastuzumab (85% *vs.* 55%, $P<0.001$). In addition, 5G9 exhibited a higher internalization rate than pertuzumab (20% *vs.* 9%, $P<0.05$), and was able to further synergize with trastuzumab to promote antigen-antibody endocytosis. The internalization rate of the combination of 5G9 and trastuzumab was higher than that of pertuzumab and trastuzumab (35% *vs.* 14%, $P<0.001$). *In vivo* animal studies demonstrated that 5G9 in combination with trastuzumab showed more potent synergistic antitumor efficacy than the combination of pertuzumab and trastuzumab.
Interpretation: 5G9, together with trastuzumab, may provide a potential opportunity for more efficacious treatment of HER2-positive cancers.
Funding: National Natural Science Foundation of China; State Key Laboratory of Analytical Chemistry for Life Science.

1. Introduction

Human epithelial growth factor receptor-2 (HER2) is a receptor tyrosine kinase and a member of the transmembrane epithelial growth factor receptor (EGFR) family, which comprises EGFR (HER1), ErbB2 (HER2), HER3 and HER4 (1, 2). HER2 is able to dimerize with itself or with other EGFR family members, thus activating downstream signal transduction pathways of tyrosine phosphorylation, and eventually resulting in the regulation of various cellular functions, including cell proliferation, differentiation, and apoptosis (3-5). HER2 is moderately expressed in normal adult tissues, where it regulates cell growth and differentiation. As a key gene of cell survival, HER2 gene amplification and overexpression of the HER2 protein have been reported in 20%–30% of breast cancer, gastric cancer and ovarian cancer cases, and correlate with greater metastatic potential and poor prognosis (6-8). Since its expression levels are relatively

Abbreviations: TRA, trastuzumab; PER, pertuzumab; TV, tumor volume; TGI, tumor growth inhibition

* Corresponding authors.
** Corresponding author at: Department of Clinical Laboratory, Jinling Hospital, State Key Laboratory of Analytical Chemistry for Life Science, School of Life Sciences, Nanjing University, Nanjing, Jiangsu, China.
E-mail addresses: lanluo@nju.edu.cn (L. Luo), mingjiu.chen@biosion.com (M. Chen), zchunni27@hotmail.com (C. Zhang).
[1] These authors contributed equally to this article.

https://doi.org/10.1016/j.ebiom.2020.102996

Research in context

Evidence before this study

The discovery of HER2-targeting monoclonal antibodies has revolutionized the treatment of HER2-positive cancers. Trastuzumab and pertuzumab are two monoclonal antibodies targeting HER2, and the combination use of trastuzumab and pertuzumab has been used as the first-line treatment for HER2 positive cancers. Because pertuzumab was primarily developed as HER2 dimerization inhibitor, and later was incidentally found to have synergistic activity with trastuzumab, it remains to know whether an optimal synergistic partner could be identified for maximizing the efficacy of trastuzumab.

Added value of this study

Here we identified trastuzumab optimal synergistic antibodies (4H2, 4C9, 4G6, 5F12 and 5G9) by large scale trastuzumab-based synergistic efficacy screening. These monoclonal antibodies bound to a unique epitope and showed similar physiochemical properties, cell-based bioactivities and *in vivo* efficacy when combining with trastuzumab. 5G9 (a representative of these antibodies) -medicated HER2 endocytosis was significantly higher than either trastuzumab- or pertuzumab- medicated endocytosis. Unlike pertuzumab, 5G9 greatly enhanced trastuzumab-medicated HER2 endocytosis, consequently resulting in the degradation of HER2 protein, the disruption of HER2-medicated cell signaling pathway, and the initiation of apoptosis. Although only showing marginal antitumor efficacy of itself, 5G9 was able to greatly promote the antitumor efficacy of trastuzumab in both *in vitro* bioassays and *in vivo* animal models, and such combinational efficacy was due to synergistic effect, rather than addition effect.

Implications of all the available evidence

Our findings of 5G9 and its optimal synergistic efficacy with trastuzumab are of great significance in anti-HER2 therapy. To our knowledge, this is the first report for discovering novel antibody drug candidates by using a blockbuster drug-based large-scale synergistic functional screening.

low in normal tissues, HER2 is an attractive target for targeted therapy (9, 10).

Anti-HER2 monoclonal antibodies were able to inhibit HER2 activity in some high expression tissues, which revolutionized the therapy of HER2-positive breast cancer patients, both in the early phase and the metastatic phase (11). To date, trastuzumab, pertuzumab and ado-trastuzumab-emtansine (T-DM1) have been approved for clinical use by the U.S. Food and Drug Administration (FDA) (12, 13). Among them, trastuzumab targets domain-IV of the HER2 extracellular domain (ECD) and shows significant efficacy in the treatment of HER2 high expression breast cancer. Pertuzumab is the second anti-HER2 antibody drug, which binds to domain-II of the HER2 ECD (14, 15). As a single agent, unlike trastuzumab, pertuzumab shows marginal antitumor activity in human patients (16). However, when pertuzumab and trastuzumab were combined together, they showed potent synergistic efficacy toward HER2-positive cancer cells *in vitro* and *in vivo* (17, 18). The subsequent clinical trials further confirmed that pertuzumab increased the efficacy of trastuzumab in patients; thus, pertuzumab was approved as a combination therapy with trastuzumab for the treatment of HER2-positive metastatic breast cancer (19-21). In addition, T-DM1, the first antibody-drug conjugate consisting of trastuzumab cross-linked with the cytotoxic maytansinoid, was approved for the treatment of HER2+ metastatic breast cancer in 2013 and for HER2+ early breast cancer in 2019, mainly based on its role in prolonging overall survival with an objective response rate of 44% (22). Based on the exciting efficacy of the pertuzumab and trastuzumab combination, it was anticipated that pertuzumab may improve the efficacy of T-DM1 as well in the treatment of HER2-positive cancer. Unexpectedly, clinical trial demonstrated that pertuzumab failed to improve the antitumor efficacy of T-DM1 in the treatment of HER2-positive advanced breast cancer (23). Although these HER2-targeting antibodies, as single agents or in combination, show encouraging efficacy in the treatment of HER2-positive breast cancer, not all patients respond to these therapies, revealing their limitation in their efficacy (24).

It has been shown that the combination of two or more monoclonal antibodies with nonoverlapping epitopes shows synergistic antitumor activity over single agents in both preclinical studies and clinical settings (25-29). Since pertuzumab was primarily developed as a HER2 dimerization inhibitor and was incidentally found to have synergistic antitumor activity with trastuzumab, it remains to be seen whether an optimal synergistic partner could be identified to maximize the anti-HER2 efficacy of trastuzumab. To explore this possibility, we performed a large-scale trastuzumab-based synergistic functional screening and identified five monoclonal antibodies (4H2, 4C9, 4G6, 5F12 and 5G9) with more potent synergistic antitumor activity than pertuzumab. Interestingly, all five monoclonal antibodies bound to a unique epitope, named trastuzumab-optimal-synergistic-epitope (TOSE), which was distinct from the trastuzumab-binding epitope or pertuzumab-binding epitope. Endocytosis studies demonstrated that 5G9 had a higher internalization rate than trastuzumab and pertuzumab, and was able to further enhance antigen-antibody internalization when combined with trastuzumab. *In vivo* animal studies demonstrated that, in combination with trastuzumab, 5G9 exhibited significantly better efficacy than pertuzumab in the treatment of both breast and gastric cancers. Overall, 5G9, an optimal synergistic partner of trastuzumab, may provide a potential therapeutic opportunity for more efficacious treatment of HER2-positive cancers.

2. Materials and methods

2.1. Cell culture and reagents

Human breast cancer cell lines (BT-474, SK-BR-3, AU-565, MDA-MB-175-VII, MCF-7) and a human gastric cancer cell line (NCI-N87) were obtained from American Type Culture Collection (ATCC). BT-474 cells (ATCC Cat# HTB-20, RRID:CVCL_0179), SK-BR-3 cells (ATCC Cat# HTB-30, RRID:CVCL_0033), MDA-MB-175-VII cells (ATCC Cat# HTB-25, RRID:CVCL_1400) and MCF-7 cells (ATCC Cat# HTB-22, RRID:CVCL_0031) were cultured in Dulbecco's modified Eagle's medium (DMEM, Gibco Cat# 10566-016). NCI-N87 cells (ATCC Cat# CRL-5822, RRID:CVCL_1603) and AU-565 cells (ATCC Cat# CRL-2351, RRID:CVCL_1074) were cultured in RPMI-1640 medium (Gibco Cat# 22400-089). All media were supplemented with 10% fetal bovine serum (FBS) (Gibco Cat# 10099-141), and cells were cultured at 37 °C and 5% CO_2.

The anti-HER2 monoclonal antibodies trastuzumab and pertuzumab were produced by Genentech Incorporated. The anti-EGFR monoclonal antibody cetuximab was produced by Merck Incorporated. The recombinant proteins huEGFR (Cat# 10001-H02H), huHER2 (Cat# 10004-H02H), huHER3 (Cat# 10201-H02H), huHER4 (Cat# 10363-H02H), rhesus HER2 (Cat# 90020-K02H) and mouse HER2 (Cat# 50714-M02H) were purchased from Sino Biological Inc. The HER/ErbB Family Antibody Samper kit (Cat# 8339, RRID: AB_10860426), phosphoplus® P44/42 ERK (Thr202/Tyr204) Antibody kit (Cat# 9100, RRID:AB_330741), phosphoplus® Akt (Ser473) Antibody kit (Cat# 9270, RRID:AB_329824), GAPDH (Cat# 2118, RRID:

AB_561053) and protease/phosphatase inhibitor cocktail (Cat# 5872) were purchased from Cell Signaling Technology.

2.2. Immunization and generation of antibody repertoires

Eight to ten-week-old BALB/c (IMSR Cat# CRL_028, RRID: IMSR_CRL:028) or A/J female mice (IMSR Cat# ARC:AJ, RRID: IMSR_ARC:AJ) were immunized with BT-474 cells and recombinant human HER2-ECD protein (Sino Biological Cat# Cat: 10004-HCCH) by the standard immunization method. Mice with a high serum titer were used for hybridoma fusions. An ELISA-based assay was used to screen HER2-positive hybridoma cell lines, which were further ranked by cell-based binding screening for hybridoma cell lines with strong binding to cells with high-level HER2 expression but low binding to cells with low-level HER2 expression. By pairing with trastuzumab (1 μg/ml), supernatants of ~600 HER2-positive hybridoma lines with strong binding activity to high-level HER2 expressing cells were subjected to a large-scale functional synergistic screening of cell proliferation inhibition by using the human breast cancer cell lines BT-474 and MDA-MB-175-VII. The synergistic bioactivity of a hybridoma supernatant (1/3 dilution) with trastuzumab was determined by dividing its combined bioactivity with either the single agent bioactivity or the combined activity of trastuzumab and pertuzumab.

2.3. ELISA and cell-based binding assay

For indirect ELISA, plates were coated with 2 μg/ml of HER2-ECD in carbonate buffer at 4 °C for 2 hours or overnight. After blocking with 5% milk at room temperature for 2 hours, the series diluted tested antibodies were added and incubated at room temperature for 2 hours, and then subjected to the detection by HRP-conjugated secondary antibodies (goat anti-human Fc, Jackson Immune Research Laboratories Cat# 109-035-003, or goat anti-mouse Fc, Jackson Immune Research Laboratories Cat# 115-035-205). After washed with PBST (Sigma-Aldrich Cat# 524653) four times, TMB (Sigma-Aldrich Cat# T0440) was added as a substrate and the absorbance detected at 405 nm.

For antibody epitope grouping, competitive ELISA was performed to determine whether two monoclonal antibodies bind to the same epitope or to distinct different epitopes. Briefly, 96-well plates were coated with 100 μl 0.5 μg/ml of testing monoclonal antibodies overnight, and then blocked by 1% BSA (Sigma-Aldrich Cat# A2058) in PBST for 1 hour at 37 °C. After four times washes with PBST, pre-incubated mixture of HER2-ECD-biotin with 10 μg/ml testing antibodies into plates and incubate for 1 hour. After four times washes with PBST, 100 μl of HRP-streptavidin (1:5000) (Sigma-Aldrich Cat# S2438) was added to each well for 1 hour at 37 °C. After washed with PBST four times, TMB was added as a substrate and the absorbance detected at 405 nm.

For cell-based binding assay, briefly, cells in exponential stage were harvested with cell dissociation buffer, and were dispensed into a 96-well (round bottom) plate at 1~5 $\times$ 10^5 cells/well and incubated with 50 μl series diluted (starting from 20 μg/ml) testing antibody (trastuzumab, pertuzumab or 5G9) at 4 °C for 1 hour. Cells were then washed 3 times with FACS buffer (PBS pH 7.2 with 2% FBS) and re-suspended in 100 μl goat anti-mouse IgG-F(ab)$_2$-Alexa (Jackson Immune Research Cat# 109-546-003). After incubation at 4 °C for 1 hour, cells were then washed 3 times with FACS buffer (PBS pH 7.2 with 2% FBS) and then re-suspended in FACS buffer followed binding signal collection and analysis by FACS instrument (FACS Calibur^{TM} Flow Cytometer, BD Bioscience).

2.4. Cell viability assay, EdU assay and cell migration assay

BT-474 cells were seeded at a preoptimized cell density in 96-well plates and precultured for 12 hours. After the cells were treated with antibodies at the indicated concentrations and cultured for 3−6 days, 25 μl of Cell Titer-Glo (Promega Cat# G7570) solution was added to each well of 96-well plates to determine cell viability. Relative cell viability was calculated by dividing the absorbance of each well by the mean absorbance of the PBS treated wells in each plate.

Cell proliferation was further examined by using an EdU assay kit (RiboBio Cat# C10310) according to the manufacturer's instructions. The percentage of EdU-positive cells was calculated by dividing the number of EdU-positive cells by the number of Hoechst-stained cells.

Cell migration ability was assessed by a wound healing assay. Briefly, BT-474 cells were cultured for 48 hours in 6-well plates and then an artificial wound was created by using a 200 μl pipette tip. Subsequently, the cells were cultured in DMEM with 5% fetal bovine serum and the indicated testing antibodies for 72 hours. To visualize the migrated cells and wound healing, images were acquired at 0 and 72 hours after the wound was created.

2.5. Cell apoptosis analysis

BT-474 cells (15,000/well) were seeded into 6-well plates and incubated with the indicated testing antibodies (100 nM). After 72 hours of antibody treatment, cells were detached with trypsin and 1 $\times$ 10^5 cells were used for analysis. For apoptosis analysis, cells were analyzed using the FITC annexin-V apoptosis detection kit (BD Cat# 556547) according to the manufacturer's instructions. Cells were analyzed on a FACS Calibur with FlowJo software.

Poly (ADP-ribose) polymerase (PARP) was measured as a marker of cell apoptosis by immunoblotting. BT-474 cells were treated with 10 μg/ml of the indicated antibodies and harvested after 3 days. Cell lysates from each treatment were subjected to SDS-PAGE and western-blot. Full length PARP (Mr 116,000) and cleaved PARP (Mr 89,000) (Cell Signaling Technology Cat# 5625, RRID:AB_10699459) were measured by immunoblotting.

2.6. Endocytosis assay

SK-BR-3 cells were trypinized and resuspended in pre-cold FACS buffer to the cell density of 3 $\times$ 10^6/ml. Resuspended cells (1 ml) were tansferred to FACS tubes and followed with addition of testing antibodies (transtuzumab, pertuzumab, or 5G9) labelled with Alexa488 (Sigma-Aldrich Cat# MX488AS20) or Alexa633 (Sigma-Aldrich Cat# MX633S100). Cells were incubated on ice for one hour and washed two times followed by dissolving cells into 1 ml FACS buffer. Aliquoted 200 μl to two new tubes labelled as time-zero (T0) group and blank control group. The remaining cells were resuspended in DMEM + 10% FBS + PS, and incubated at 37 °C for 30 min or 2 hours, and then 200 μl of cells were transferred to new tube pre-incubated in ice for 5 min, washed one time by FACS buffer. All tubes except T0 group were added 250 μl stripping buffer and then incubated at room temperature. All tubes were added 200 μl fixing buffer and incubated at 4 °C for 30 min before measuring the mean fluorescence intensity (MFI) of each treated group. T0 group represents maximum cell surface binding of each labelled antibody while blank control group represents the background binding of each labelled antibody without 37 °C incubation. Internalization rate = $(MFI^{test} - MFI^{blank})/(MFI^{T0} - MFI^{blank}) \times 100\%$.

2.7. HER2-mediated cell signaling pathways

Cells (20,000/well) were seeded into 6-well plates and incubated with different antibodies (100 nM each antibody). After 3 days of treatment, cells were washed with ice-cold PBS and lysed in cell lysis solution [50 mM Tris, pH 7.4, 150 mM NaCl, 1% NP-40, 0.1% sodium dodecyl sulfate, 1 mM NaF, 1 mM Na_3VO_4, 1 mM PMSF, and protease inhibitor cocktail (Sigma-Aldrich Cat# P8340)]. Immunoblotting was conducted using NuPAGE gels (Genescript Cat# M00652) according

to the manufacturer's instructions with anti-HER2, anti-pHER2 (Y1221/1222), anti-EGFR, anti-pEGFR (Y1068), anti-HER3, anti-pHER3 (Y1289), anti-ERK, anti-pERK (T202/T204), anti-AKT, anti-pAKT (S473) and anti-GAPDH antibodies (Cell Signaling Technology). Horseradish peroxidase-conjugated anti-mouse (Cat# 7076, RRID: AB_330924) and anti-rabbit antibodies (Cat# 7074, RRID: AB_2099233) were purchased from Cell Signaling Technology. Bands were visualized using Tanon 5200.

2.8. ADCC assays

SE Cell Line4D-NucleofectorTM X Kit L (Lonza Cat #: PBC1-02250) was used to construct the effect cell line (Jurkat-NFAT-CD16) according to manufacture operating instructions. To perform the assay, 50 μl of target cells (BT-474 or NCI-N87, 2×10^5 cells/ ml) was added to each well of a 96-well plate followed with the addition of 50 μl of serial dilutions (initial concentration 400 nM) of either trastuzumab, pertuzumab or hu5G9 (a humanized version of 5G9 with the same IgG1-Fc as trastuzumab or pertuzumab). To test the combination of trastuzumab plus pertuzumab or hu5G9, 50 μl of antibody mixture (1:1) was added instead. Thus, the final total concentration of the antibody mixture was the same as in the single antibody experiments. After incubation for 1 hour at 37 °C, 100 μl of effector cell Jurkat-NFAT-CD16 (6×10^5 cells/ ml) was added, and continued to incubate for 6 hours. The ratio of effector cell to target cell was 6:1. MCF-7 and HEK293T (ATCC Cat# CRL-3216, RRID:CVCL_0063) were used as negative control cell lines. huIgG was used as negative control antibody. The relative luminescence activity was measured by luciferase assay system.

2.9. In vivo *animal model studies*

A total of 1×10^6 NCI-N87 cells and 5×10^6 BT-474 cells were inoculated subcutaneously into the right flank of 6 to 8-week-old NOD SCID mice (IMSR Cat# CRL:394, RRID:IMSR_CRL:394). Tumors were allowed to grow to approximately 200 mm^3 or 500 mm^3 in size, and then mice were randomized into groups. Animals received intraperitoneal administration of antibodies at the indicated doses twice weekly. Tumor volumes were calculated using the formula $(L \times W \times W)/2$, where "L" represents the larger tumor diameter and "W" represents the smallest tumor diameter. Animals were sacrificed, and the tumors were isolated and weighed after the termination of the studies. Animals in the study group were also sacrificed if the average tumor volume was >3000 mm^3.

2.10. Ethical statement

All animal experiments were performed according to institutional guidelines of Crown Bioscience. All protocols with animal experimentation conformed to criteria outlined in the National Institutes of Health "Guide for the Care and Use of Laboratory Animals." Protocols were reviewed and approved by the animal use committee of Crown Bioscience (protocal number: AN-1407-009-133).

2.11. Statistical analysis

Experimental data were determined using one-way or two-way ANOVA with the Bonferroni correction. Significance levels were set at a P value less than 0.05. All analyses were performed using GraphPad Prism 7 software.

3. Results

3.1. All TOSE-binding antibodies bind to a unique epitope distinct from the trastuzumab-binding epitope or pertuzumab-binding epitope

To identify monoclonal antibodies with maximal trastuzumab-synergistic antitumor efficacy, mice immunized with human breast cancer BT-474 cells and recombinant human HER2-ECD protein were used for hybridoma fusion experiments to create a large pool of target-specific hybridoma cell lines. As a result, 1175 HER2-positive hybridomas were identified in an ELISA-based screening. Among them, 24 hybridoma supernatants bound to the trastuzumab-binding epitope (data not shown), and 2 supernatants bound to the pertuzumab-binding epitope (data not shown), indicating that all potential HER2-ECD epitopes may be covered by the pool of 1175 HER2-positive hybridomas. After one round of cell-based binding screening, the top 600 hybridoma supernatants with strong HER2 cell-binding activity were identified and subsequently subjected to a large-scale trastuzumab-based cell proliferation inhibition screening by using the human breast cancer cell lines BT-474 and MDA-MB-175-VII (data not shown), which lead to five monoclonal antibodies (4H2, 4C9, 4G6, 5F12 and 5G9) with the highest trastuzumab-based synergistic bioactivity (Fig. 1a). The superior trastuzumab-based synergistic bioactivity of the resultant five monoclonal antibodies was further validated by using purified antibodies, confirming that each of the five antibodies indeed exhibited more potent trastuzumab-based synergistic activity than pertuzumab (Fig. 1b). Interestingly, an epitope grouping assay revealed that all five monoclonal antibodies bound to a unique epitope - (called trastuzumab-optimal-synergistic-epitope, TOSE) - that was distinct from both the trastuzumab-binding epitope and pertuzumab-binding epitope (Fig. 1c).

Similar to trastuzumab and pertuzumab, all TOSE-binding antibodies specifically bound to HER2 protein but not other EGFR family members including EGFR, HER3 or HER4 (Fig. 1d). TOSE-binding antibodies were able to bind monkey HER2 protein but not murine HER2 proteins (Fig. 1e). Moreover, TOSE-binding antibodies recognized the high HER2 expression cell lines (BT-474 and SK-BR-3) but not the low HER2 expression cell line MCF-7 (Supplementary Fig. S1).

3.2. 5G9 and trastuzumab synergistically inhibit HER2-positive cancer cell growth

To investigate that the combined efficacy of trastuzumab and 5G9 (a representative of the TOSE-binding antibodies) is due to a synergistic but not additive effect, BT-474 cells were treated in triplicate with 3-fold serial dilutions of trastuzumab, pertuzumab, 5G9 or the combination of trastuzumab with either pertuzumab or 5G9 at a 1:1 fixed dose ratio. The inhibition of cell viability was examined by Cell Titer Glo after 6 days of treatment, and was calculated as the percentage of viable cells in each treated group relative to the untreated group. 5G9 or trastuzumab exhibited weak or moderate inhibition of cell proliferation in the BT-474 cell-based assay; however, the combination of trastuzumab and 5G9 at the same dosage showed substantially enhanced inhibition of cell proliferation compared to single agents (Fig. 2a). More importantly, the cell proliferation inhibitory activity of trastuzumab and 5G9 was significantly higher than that of trastuzumab and pertuzumab, suggesting that 5G9 is a more potent synergistic partner for trastuzumab than pertuzumab.

Based on the above cell proliferation inhibition assay, the synergism between trastuzumab and 5G9 was further analyzed by using the method of Chou and Talalay to calculate the drug combination index (CI.) values (Fig. 2b). As indicated in Fig. 2b, the CI value of the combination of 5G9 and trastuzumab was lower than that of the

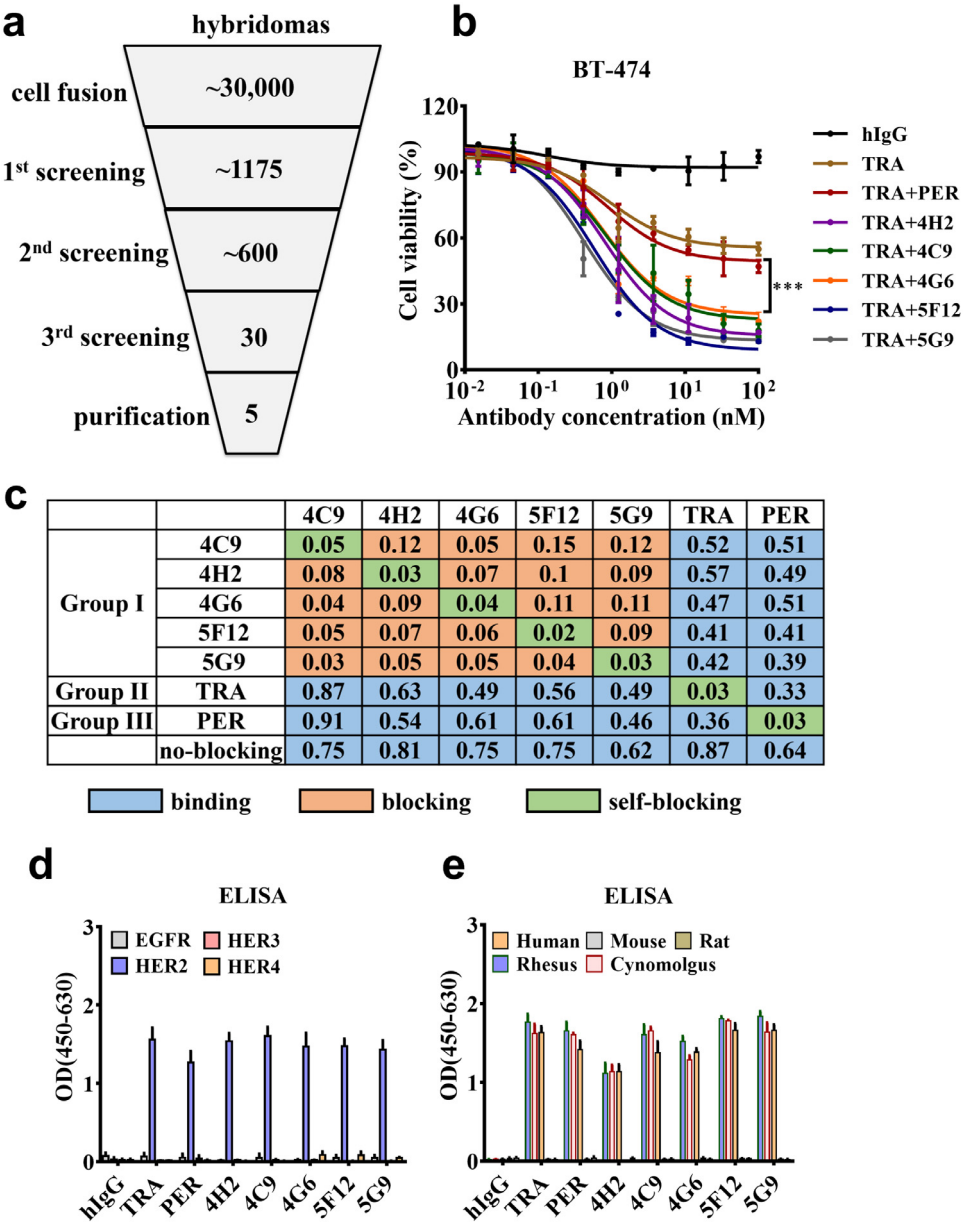

Fig. 1. Characterization of trastuzumab-optimal-synergistic-epitope (TOSE) -binding monoclonal antibodies. (a) Schematic workflow of trastuzumab-based synergistic functional screening of TOSE-binding antibodies (4H2, 4C9, 4G6, 5F12 and 5G9). 1st screening: ELISA binding and competitive ELISA with trastuzumab or pertuzumab; 2nd screening: binding to HER2-positive cells; 3rd screening: trastuzumab-based cell proliferation inhibition assay. (b) Five monoclonal antibodies (4H2, 4C9, 4G6, 5F12 and 5G9) showed trastuzumab-synergistic bioactivity higher than pertuzumab in the BT-474 cell proliferation inhibition assay. TRA: trastuzumab; PER: pertuzumab. (c) The antibody epitope grouping assay was performed by competitive ELISA. Five monoclonal antibodies (4H2, 4C9, 4G6, 5F12 and 5G9) bound to a unique epitope-TOSE, which was different from both the trastuzumab-binding epitope and pertuzumab-binding epitope. (d) The binding specificity and species cross-reactivity were determined by ELISA. 5G9 bound to HER2 protein, but not to other EGFR family members, including EGFR, HER3 and HER4. (e) The cross-species binding reactivity was determined by ELISA. 5G9 was able to bind cynomolgus HER2 protein but not murine HER2 protein. The BT-474 cell proliferation inhibition assay, antibody epitope grouping assay and the cross-reactivity assay were repeated three times and the results were shown as the mean ± SD ($n = 3$). Two-way ANOVA, $^{***}P<0.001$.

combination of trastuzumab and pertuzumab (ED_{50}: 0.211 vs. 0.322; ED_{75}: 0.385 vs. 0.455; ED_{90}: 0.773 vs. 0.789), indicating that the synergism between 5G9 and trastuzumab was stronger than that of pertuzumab and trastuzumab.

In support of the above findings, the potent inhibition of proliferation was confirmed by EdU assay, and the number of living cells or cells in the proliferating state was significantly decreased in cells treated with the combination of trastuzumab plus 5G9 compared to cells treated with single agents or the combination of trastuzumab plus pertuzumab (Fig. 2c).

In line with the above results, the superior synergism between trastuzumab and 5G9 was also demonstrated in cell proliferation assays by using other HER2 positive cell lines including NCI-N87, SK-BR-3, and AU-565 (Fig. 2d). The combined efficacy of trastuzumab and 5G9 was about 10~22% higher than that of trastuzumab and pertuzumab (NCI-N87: 66% *vs.* 40%; SK-BR-3: 62% *vs.* 53%; AU-565: 54% *vs.* 43%) although the efficacy of 5G9 and pertuzumab was quite similar (NCI-N87: 73% *vs.* 61%; SK-BR-3: 82% *vs.* 81%; AU-565: 70% *vs.* 70%). Furthermore, wound healing assays with BT-474 cells revealed that 5G9 in combination with trastuzumab showed significantly stronger inhibitory activity on cell migration than either single agent or the combination of trastuzumab plus pertuzumab (Supplementary Fig. S2), consistent with the above findings. Taken together, our results demonstrate that 5G9 is a more potent trastuzumab-synergistic efficacy partner than pertuzumab.

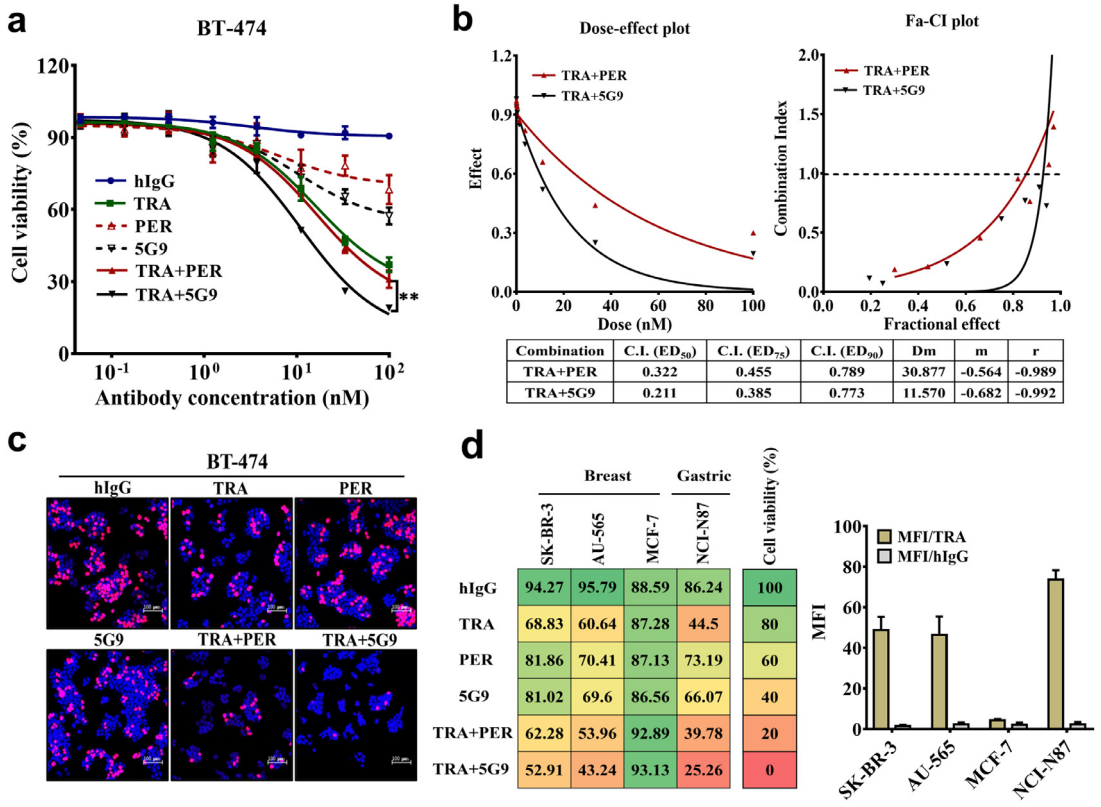

Fig. 2. 5G9 and trastuzumab synergistically inhibit HER2-positive cancer cell growth. (a) Inhibition of BT-474 cell viability was examined by Cell Titer Glo after 6 days of antibody treatment. The initial antibody concentration was 100 nM for both the monoclonal antibody and the antibody combination (1:1 ratio). Growth inhibition was calculated as the fraction of viable cells in the antibody treated group compared with untreated control cells. The cell proliferation inhibition assay was repeated three times and the results were shown as the mean ± SD (n = 3). Two-way ANOVA, $^{**}P<0.01$. TRA: trastuzumab; PER: pertuzumab. (b) Dose-effect plots and combination index (CI.) plots of the two combinations were calculated by using the method of Chou and Talalay with the commercial software Calcusyn. C.I. values for effective doses at which 50%, 75%, and 90% (ED_{50}, ED_{75}, and ED_{90}, respectively) of cells were killed. Drug synergy was defined by C.I. values less than 1, the lower C.I. value, the more synergy. (c) Representative images from the EdU assay of BT-474 cells. The viable cells were stained blue by DAPI (blue) and the proliferation cells were stained red by EdU (red).The EdU assay was repeated three times and the representative images were shown. (d) Human breast cancer cell lines (SK-BR-3, AU-565, MCF-7) and human gastric cell lines (NCI-N87) were treated with 100 nM antibodies for 3 or 6 days and cell viability was determined by Cell Titer Glo. The experiments were repeated three times and the cell viability is shown as the mean ± SD (n = 3). The relative HER2 expression of cell lines was detected and analyzed by flow cytometry and FlowJo software.

3.3. The combination of trastuzumab plus 5G9 more efficiently enhances cell apoptosis, HER2 internalization and cell signaling pathway blocking

To investigate the mechanism of action of the antiproliferative synergistic activity of 5G9 in combination with trastuzumab, cells were treated with single agents (trastuzumab, pertuzumab, 5G9 or IgG control) or combinations (trastuzumab plus pertuzumab or trastuzumab plus 5G9) for 3 days and then stained with PI to measure cell death and with annexin-V for early apoptosis. As shown in Fig. 3a, the number of viable cells was significantly lower in the group treated with trastuzumab plus 5G9 than in the group treated with trastuzumab plus pertuzumab ($P<0.05$), and the enhanced cell death was due to increased late-stage apoptosis (Fig. 3a, $P<0.05$). To confirm that the cytotoxic effect of 5G9 is indeed mediated by the induction of apoptosis, the protein levels of full-length and cleaved PARP were examined in BT-474 cells treated with single agents or combinations. Our results indicated significantly increased apoptosis in cells treated with the combination of trastuzumab plus 5G9, but not in cells treated with the combination of trastuzumab plus pertuzumab (Fig. 3b, Supplementary Fig. S3a and Fig. S4a, $P<0.05$).

It is known that antigen-antibody lattice formation induced by a combination of noncompeting antibodies could lead to more efficient receptor internalization for degradation (30, 31). To investigate the internalization activity of 5G9 and whether 5G9 could further enhance antigen-antibody complex internalization when combining with trastuzumab, we treated SK-BR-3 cells with either monoclonal antibodies or the combination of monoclonal antibodies. Our results first showed that the internalization rate of 5G9 was approximately two-fold higher than that of pertuzumab or trastuzumab (Fig. 3c, $P<0.05$). Unlike pertuzumab, 5G9 was able to markedly enhance the internalization rate of trastuzumab in a reciprocal way (Fig. 3d and 3e, $P<0.001$). Similarly, a significant high internalization rate and enhancement of trastuzumab internalization were observed in other TOSE-binding antibodies (Supplementary Table 1, Table 2 and Table 3). Because HER2-antibody internalization could lead to target degradation and cell signaling pathway disruption, we further investigated whether HER2-mediated signaling pathways could be affected by the treatment of the combination of trastuzumab plus 5G9. Extracts prepared from BT-474 cells treated with single or the combination of monoclonal antibodies were subjected to western blotting using the antibodies anti-EGFR, anti-HER2, anti-HER3, anti-ERK and anti-AKT. Our results demonstrated that the total HER2 protein level and phosphorylated HER2 level were lower in cells treated with the antibody combination than in cells treated with single agents. Consequently, the levels of p-EGFR, p-HER3, p-AKT and p-ERK were also down-regulated in cells treated with the antibody combination, although the total level of each protein was not altered (Fig. 3f, Supplementary Fig. S3b - S3f and Fig. S4b - S4f). Nevertheless, our results did not show significantly different cell signaling pathway blocking activity between 5G9 and pertuzumab, in combination with trastuzumab, most likely due to the poor sensitivity of western blots. Overall, the internalization rate of the combination of trastuzumab plus 5G9 was significantly higher than that of trastuzumab plus pertuzumab, implying more efficient HER2 internalization for

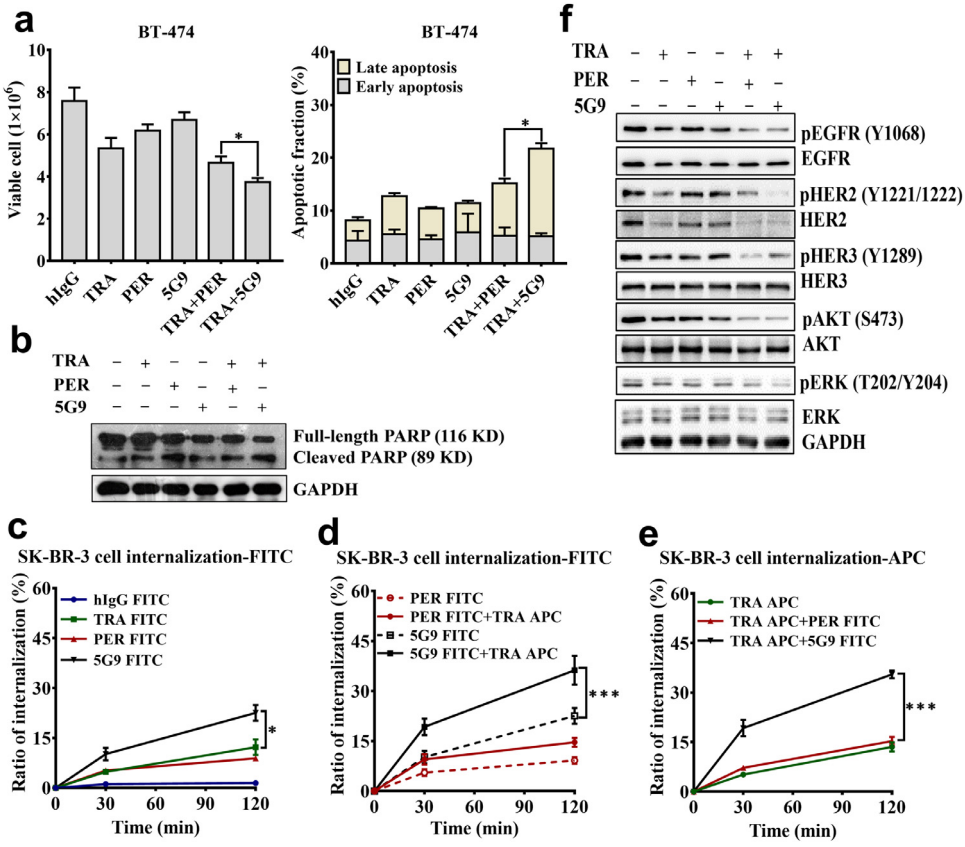

Fig. 3. 5G9 and trastuzumab enhance cell apoptosis, HER2 internalization and disruption. (a) BT-474 cells were treated with 100 nM antibodies for 3 days. The number of viable cells was detected by Trypan Blue, and annexin-V and PI were used to stain early apoptotic cells and dead cells. TRA: trastuzumab; PER: pertuzumab. (b) BT-474 cells were treated with 100 nM antibodies for 3 days, and cell lysates were obtained and immunoblotted with a poly (ADP-ribose) polymerase (PARP) polyclonal antibody. Cleaved PARP is represented by 89 KD-fragments and full-length PARP (116 KD). (c) HER2 internalization induced by 5G9, trastuzumab or pertuzumab in SK-BR-3 cells. (d) The effect of trastuzumab on the internalization of 5G9 or pertuzumab in SK-BR-3 cells. FITClabeled 5G9 or pertuzumab was detected and analyzed by flow cytometry and FlowJo software. (e) The effect of 5G9 or pertuzumab on the internalization of trastuzumab in SK-BR-3 cells. APC labeled trastuzumab was detected and analyzed by flow cytometry and FlowJo software. (f) Effect of HER2 single agents or combination on receptor phosphorylation and downstream signaling cascade. BT-474 cells were treated with 100 nM antibodies for 3 days, and cell lysates were obtained and immunoblotted with antibodies against EGFR, p-EGFR, HER2, p-HER2, HER3, p-HER3, AKT, p-AKT, ERK, p-ERK, and GAPDH. All experiments were repeated three times and the representative images and data were shown. Two-way ANOVA, $^{*}P<0.05$, $^{***}P<0.001$.

degradation, thus triggering cell apoptosis and cell signaling pathway blocking and subsequently resulting in cell growth inhibition.

Since both pertuzumab and trastuzumab can evoke antibody-dependent cellular cytotoxicity (ADCC) as one of mechanism of action for anti-HER2 therapy (32, 33), we also performed experiments to evaluate ADCC activity for trastuzumab, pertuzumab, hu5G9 (a humanized version of 5G9 with the same IgG1-Fc as trastuzumab and pertuzumab), and the combination of monoclonal antibodies. Our results demonstrated that hu5G9 evoked a similar ADCC as trastuzumab or pertuzumab. Our results further demonstrated either the combination of pertuzumab and trastuzumab or that of hu5G9 and trastuzumab did not show significantly stronger ADCC than single monoclonal antibody in both BT-474 cells and NCI-N87 cells (Supplementary Fig. S5).

3.4. *5G9 in combination with trastuzumab shows potent synergistic antitumor efficacy* in vivo

To confirm the *in vivo* synergistic antitumor activity of 5G9 and trastuzumab, we compared the tumor size in NCI-N87 tumor xenograft mice treated with 5G9, trastuzumab or their combination. Compared to PBS treatment, the low dose (5 mg/kg) treatment with trastuzumab exhibited potent antitumor *in vivo* efficacy (Fig. 4a, TGI: 56.10%, $P<0.01$) while the low dose (5 mg/kg) treatment with 5G9 only showed marginal antitumor *in vivo* efficacy (Fig. 4a, TGI: 18.16%). As expected, the combination of trastuzumab plus 5G9 at a low dose (5 mg/kg + 5 mg/kg) demonstrated significantly higher antitumor efficacy (TGI: 98%) than trastuzumab alone even at a higher dose (15 mg/kg, TGI: 63%, $P<0.001$), implying that strong *in vivo* efficacy synergism indeed exists between trastuzumab and 5G9. In combination with trastuzumab at low dose treatment (5 mg/kg + 5 mg/kg), 5G9 was able to significantly enhance the antitumor efficacy of trastuzumab (TV^{D22}=8.75 ± 4.25, $P<0.01$, TGI: 98.31%) than pertuzumab (TV^{D22}= 46.83 ± 14.48, TGI: 90.97%) (Fig. 4b). More significantly, at a high dose treatment (15 mg/kg + 15 mg/kg), tumors were completely eradicated in six out of seven mice treated with the combination of 5G9 and trastuzumab while tumor regression was still observed in mice treated with the combination of pertuzumab and trastuzumab (Fig. 4c). Consistent with the findings with 5G9, a similar antitumor efficacy pattern was also observed for 5F12 (Supplementary Fig. S6a, S6b and S6c), another member of the TOSE-binding antibodies, indicating that such trastuzumab-based synergistic antitumor efficacy could be a common characteristic of TOSE-binding antibodies. To further evaluate the combined synergistic antitumor efficacy of 5G9 or pertuzumab, in combination with trastuzumab, a BT-474 breast cancer xenograft model was employed. Consistent with the findings in the gastric model, 5G9 significantly enhanced the trastuzumab's antitumor efficacy of trastuzumab compared with pertuzumab (Fig. 5a, TGI: 47% *vs.* 24%, $P<0.001$). A similar antitumor efficacy pattern was also observed for 5F12 (Supplementary Fig. S7).

Overall, the *in vivo* animal models demonstrated that 5G9 has potent synergistic antitumor efficacy when combined with

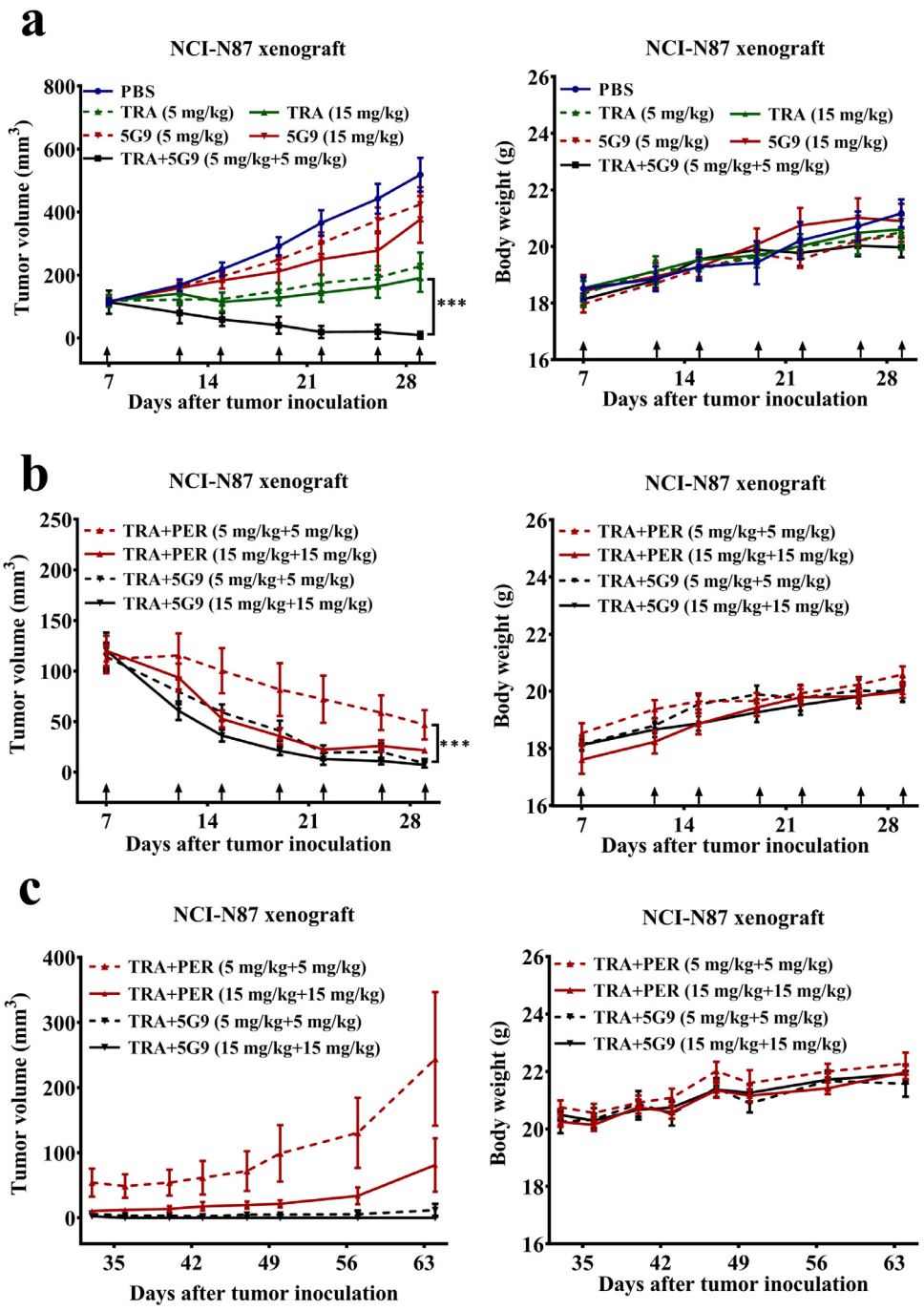

Fig. 4. ***In vivo*** **efficacy of 5G9 in combination with trastuzumab in a NCI-N87 xenograft gastric model.** (a-c) *In vivo* efficacy of 5G9 in combination with trastuzumab in the NCI-N87 xenograft gastric model. (a) *In vivo* efficacy synergism of 5G9 and trastuzumab. Mice bearing NCI-N87 tumors were randomly divided into 6 groups (n = 7, per group) and treated with PBS, TRA (5 mg/kg or 15 mg/kg), 5G9 (5 mg/kg or 15 mg/kg) or TRA ++5G9 (5 mg/kg ++5 mg/kg). Tumor volume and animal body weight were shown as the mean ± SEM (n = 7). Administration days are indicated by arrows. TRA: trastuzumab; PER: pertuzumab. (b) Superior efficacy of the combination of 5G9 and trastuzumab. Mice bearing NCI-N87 tumors were randomly divided into 4 groups (n = 7, per group) and treated with PBS, TRA+PER (5 mg/kg ++5 mg/kg), TRA ++PER (15 mg/kg ++15 mg/kg), TRA ++5G9 (5 mg/kg + +5 mg/kg) or TRA ++5G9 (15 mg/kg ++15 mg/kg). Tumor volume and animal body weight were shown as the mean ± SEM (n = 7), respectively. Administration days were indicated by arrows. (c) Tumor regression in animal treated with the combination of trastuzumab plus either 5G9 or pertuzumab. After the end of treatment on day 29, tumor growth in animal treated in different group was continuously observed and measured from day 29 to day 64. Tumor volume and animal body weight were shown as the mean ± SEM (n = 7), respectively. Two-way ANOVA, ***P<0.001. Administration days were indicated by arrows.

trastuzumab although it showed weak antitumor activity by itself, and exhibited superior synergistic efficacy with trastuzumab compared to pertuzumab.

4. Discussion

To explore the possibility of identifying an optimal functional partner for trastuzumab, the present study initiated a large-scale trastuzumab-based synergistic functional screening, which identified five monoclonal antibodies (4H2, 4C9, 4G6, 5F12 and 5G9) with superior trastuzumab-synergistic antitumor activity to pertuzumab. Further studies showed that all five monoclonal antibodies had similar biochemical characteristics, *in vitro* bioactivities and *in vivo* efficacy, indicating that the synergistic efficacy of 5G9 and trastuzumab was most likely due to the synergy between TOSE- and trastuzumab-binding epitope. It is known that the synergistic bioactivity could be

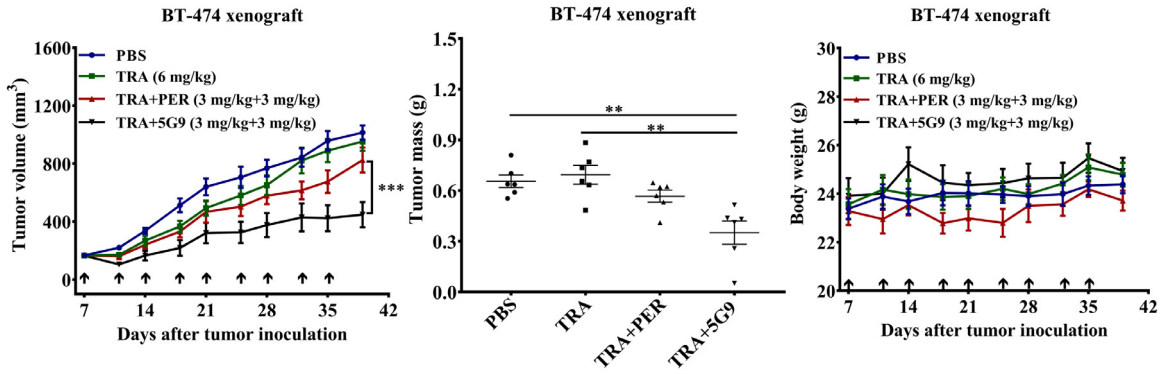

Fig. 5. ***In vivo* efficacy of 5G9 in combination with trastuzumab in a BT-474 xenograft breast model.** *In vivo* efficacy of 5G9 in combination with trastuzumab in BT-474 xenograft mice model. Mice were inoculated subcutaneously with 3×10^6 BT-474 cells on day 0. Trastuzumab (6 mg/kg) alone, the combination of trastuzumab plus 5G9 (3 mg/kg ++3 mg/kg), and the combination of trastuzumab plus pertuzumab (3 mg/kg ++3 mg/kg) were injected intravenously on day 7. PBS was used as vehicle control. Tumor volume and animal body weight were shown as the mean ± SEM (n = 6), respectively. Two-way ANOVA, $^{***}P<0.001$. Administration days were indicated by arrows.

significantly different for the combination of antibodies binding different epitopes (28), to trastuzumab-binding epitope, TOSE showed significantly better synergistic efficacy than the pertuzumab-binding epitope. Overall, we conclude that TOSE is the optimal functional synergistic epitope for the trastuzumab-binding epitope and that TOSE-binding antibodies are optimal functional partners of trastuzumab.

It is known that a combination of noncompeting antibodies targeting the HER2 family receptor shows more potent antitumor activity than single monoclonal antibodies *in vitro* and *in vivo* (34-36). In addition, trastuzumab in combination with different anti-HER2 monoclonal antibodies exhibited differential antitumor activities *in vitro* and *in vivo* (33, 37, 38). To explain the more potent antitumor efficacy of the combinational treatment of trastuzumab plus 5G9 than that of trastuzumab plus pertuzumab, we speculated that HER2-related mechanisms were disrupted more efficiently in cells treated with the combination of trastuzumab plus 5G9. Indeed, HER2-related mechanisms including apoptosis and antigen-antibody complex endocytosis have been more efficiently disrupted in the combinational treatment of trastuzumab plus 5G9 than in trastuzumab plus pertuzumab. Notably, 5G9 exhibited high antibody-mediated HER2 endocytosis, that was approximately two times higher than trastuzumab or pertuzumab. Unlike pertuzumab, 5G9 was able to significantly enhance trastuzumab-mediated HER2 endocytosis and *vice versa*. It has been reported that noncompeting antibodies cross-linking receptor clustering formation at the cell surface can result in more efficient receptor internalization and lysosomal degradation than single monoclonal antibodies (39). Overall, the enhanced antibody-mediated HER2 endocytosis is likely the key mechanism of action to explain the superior antitumor activity of the combination of trastuzumab and 5G9.

In the NCI-N87 gastric model, the low dosage (5 mg/kg + 5 mg/kg) of the combination of trastuzumab plus 5G9 resulted in significantly better efficacy than treatment with a high dosage of trastuzumab (15 mg/kg) or 5G9 (15 mg/kg), indicating that strong *in vivo* synergy indeed exists between trastuzumab and 5G9. Under the same dosage, the combination of trastuzumab and 5G9 exhibited significantly better efficacy than trastuzumab and pertuzumab in both gastric and breast cancer models. Furthermore, a significant tumor progression was observed after treatment with combination of trastuzumab plus pertuzumab, but not after treatment with combination of trastuzumab plus 5G9, implying that 5G9 could provide a big potential clinical benefit if used with trastuzumab in the clinic. Consistent with the findings with 5G9, similar results were observed by using 5F12, another member of TOSE-binding antibodies, indicating that the efficacious synergy of the TOSE-binding antibodies and trastuzumab was generated by simultaneously targeting both the TOSE and trastuzumab-binding epitope. In conclusion, 5G9 is expected to be an optimal therapeutic strategy for the more efficacious treatment of HER2-positive breast cancer and HER2 overexpressing gastric cancer.

Currently, all antibody drug-related therapeutic targets except HER2 are targeted by monoclonal antibodies but not by a combination of monoclonal antibodies to different epitopes. Based on our findings, and those of others, it is anticipated that antibodies combined with optimal epitope targeting could be an important strategy for improving the clinical efficacy of current monoclonal antibody therapies.

Acknowledgments

We are grateful to Hongyan Li, Ying Xu, Wen Lu and Liangming Huang for their technical support in antibody screening. This work was supported in part by grants from National Natural Science Foundation of China (no. 81472021 and no. 81672102) and from the State Key Laboratory of Analytical Chemistry for Life Science (no. 5431ZZXM1907). These funders had no role on study design, data collection, data analysis, data interpretation or any aspect pertinent to the study. This work was also supported in part by Biosion Inc., which has certain roles on study design, data collection, data analysis, interpretation and writing of the report. We had full access to all the data in the study and had final responsibility for the decision to submit for publication.

Declaration of Competing Interests

X.H., S.X., J.L., and M.C. are employees of Biosion Inc. These authors receive compensations and stocks of Biosion Inc. Dr. Mingjiu Chen has a pending patent on Erbb2 antibodies and uses therefore (US20200002434A1). The remaining authors declare no competing interests.

Author Contributions

M.C., C. Z. and L.L organized the project. X.D., W.G. and Y.Z conducted most experiments and collected the data. X.D, X.H., S. X. and J. L. did the data analysis and interpretation. All authors reviewed the report and approved the final version.

Supplementary materials

Supplementary material associated with this article can be found, in the online version, at doi:10.1016/j.ebiom.2020.102996.

References

[1] Akiyama T, Kadooka T, Ogawara H, Sakakibara S. Characterization of the epidermal growth factor receptor and the erbB oncogene product by site-specific antibodies. Arch Biochem Biophys 1986;245(2):531–6.
[2] Rubin I, Yarden Y. The basic biology of HER2. Ann Oncol 2001;12(Suppl 1):S3–8.
[3] Yarden Y. Biology of HER2 and its importance in breast cancer. Oncology 2001;61 (Suppl 2):1–13.
[4] Tagliabue E, Balsari A, Campiglio M, Pupa SM. HER2 as a target for breast cancer therapy. Expert Opin Biol Ther 2010;10(5):711–24.
[5] Roskoski Jr. R. ErbB/HER protein-tyrosine kinases: structures and small molecule inhibitors. Pharmacol Res 2014;87:42–59.
[6] King I, Sartorelli AC. Epidermal growth factor receptor gene expression, protein kinase activity, and terminal differentiation of human malignant epidermal cells. Cancer Res 1989;49(20):5677–81.
[7] Slamon DJ, Godolphin W, Jones LA, Holt JA, Wong SG, Keith DE, et al. Studies of the HER-2/neu proto-oncogene in human breast and ovarian cancer. Science 1989;244(4905):707–12.
[8] Slamon DJ, Clark GM, Wong SG, Levin WJ, Ullrich A, McGuire WL. Human breast cancer: correlation of relapse and survival with amplification of the HER-2/neu oncogene. Science 1987;235(4785):177–82.
[9] Drebin JA, Link VC, Weinberg RA, Greene MI. Inhibition of tumor growth by a monoclonal antibody reactive with an oncogene-encoded tumor antigen. Proc Natl Acad Sci U S A 1986;83(23):9129–33.
[10] Meric-Bernstam F, Johnson AM, Dumbrava EEI, Raghav K, Balaji K, Bhatt M, et al. Advances in HER2-targeted therapy: novel agents and opportunities beyond breast and gastric cancer. Clin Cancer Res 2019;25(7):2033–41.
[11] Venter DJ, Tuzi NL, Kumar S, Gullick WJ. Overexpression of the c-erbB-2 oncoprotein in human breast carcinomas: immunohistological assessment correlates with gene amplification. Lancet 1987;2(8550):69–72.
[12] Li JY, Perry SR, Muniz-Medina V, Wang X, Wetzel LK, Rebelatto MC, et al. A biparatopic HER2-targeting antibody-drug conjugate induces tumor regression in primary models refractory to or ineligible for HER2-targeted therapy. Cancer Cell 2016;29(1):117–29.
[13] Pegram MD, Miles D, Tsui CK, Zong Y. HER2-overexpressing/amplified breast cancer as a testing ground for antibody-drug conjugate drug development in solid tumors. Clin Cancer Res 2019.
[14] Franklin MC, Carey KD, Vajdos FF, Leahy DJ, de Vos AM, Sliwkowski MX. Insights into ErbB signaling from the structure of the ErbB2-pertuzumab complex. Cancer Cell 2004;5(4):317–28.
[15] Metzger-Filho O, Winer EP, Krop I. Pertuzumab: optimizing HER2 blockade. Clin Cancer Res 2013;19(20):5552–6.
[16] Hubalek M, Brantner C, Marth C. Role of pertuzumab in the treatment of HER2-positive breast cancer. Breast Cancer (Dove Med Press 2012;4:65–73.
[17] Nahta R, Hung MC, Esteva FJ. The HER-2-targeting antibodies trastuzumab and pertuzumab synergistically inhibit the survival of breast cancer cells. Cancer Res 2004;64(7):2343–6.
[18] Howie LJ, Scher NS, Amiri-Kordestani L, Zhang L, King-Kallimanis BL, Choudhry Y, et al. FDA approval summary: pertuzumab for adjuvant treatment of HER2-positive early breast cancer. Clin Cancer Res 2019;25(10):2949–55.
[19] Baselga J, Cortes J, Kim SB, Im SA, Hegg R, Im YH, et al. Pertuzumab plus trastuzumab plus docetaxel for metastatic breast cancer. N Engl J Med 2012;366(2):109–19.
[20] Blumenthal GM, Scher NS, Cortazar P, Chattopadhyay S, Tang S, Song P, et al. First FDA approval of dual anti-HER2 regimen: pertuzumab in combination with trastuzumab and docetaxel for HER2-positive metastatic breast cancer. Clin Cancer Res 2013;19(18):4911–6.
[21] Amiri-Kordestani L, Wedam S, Zhang L, Tang S, Tilley A, Ibrahim A, et al. First FDA approval of neoadjuvant therapy for breast cancer: pertuzumab for the treatment of patients with HER2-positive breast cancer. Clin Cancer Res 2014;20(21):5359–64.
[22] Wong DJ, Hurvitz SA. Recent advances in the development of anti-HER2 antibodies and antibody-drug conjugates. Ann Transl Med 2014;2(12):122.
[23] Perez EA, Barrios C, Eiermann W, Toi M, Im YH, Conte P, et al. Trastuzumab emtansine with or without pertuzumab versus trastuzumab plus taxane for human epidermal growth factor receptor 2-positive, advanced breast cancer: primary results from the phase III MARIANNE study. J Clin Oncol 2017;35(2):141–8.
[24] Verma S, Miles D, Gianni L, Krop IE, Welslau M, Baselga J, et al. Trastuzumab emtansine for HER2-positive advanced breast cancer. N Engl J Med 2012;367 (19):1783–91.
[25] Baselga J, Swain SM. CLEOPATRA: a phase III evaluation of pertuzumab and trastuzumab for HER2-positive metastatic breast cancer. Clin Breast Cancer 2010;10 (6):489–91.
[26] Scheuer W, Friess T, Burtscher H, Bossenmaier B, Endl J, Hasmann M. Strongly enhanced antitumor activity of trastuzumab and pertuzumab combination treatment on HER2-positive human xenograft tumor models. Cancer Res 2009;69 (24):9330–6.
[27] Friedman LM, Rinon A, Schechter B, Lyass L, Lavi S, Bacus SS, et al. Synergistic down-regulation of receptor tyrosine kinases by combinations of mAbs: implications for cancer immunotherapy. Proc Natl Acad Sci U S A 2005;102(6):1915–20.
[28] Koefoed K, Steinaa L, Soderberg JN, Kjaer I, Jacobsen HJ, Meijer PJ, et al. Rational identification of an optimal antibody mixture for targeting the epidermal growth factor receptor. MAbs 2011;3(6):584–95.
[29] Abramson V, Arteaga CL. New strategies in HER2-overexpressing breast cancer: many combinations of targeted drugs available. Clin Cancer Res 2011;17(5):952–8.
[30] Ben-Kasus T, Schechter B, Lavi S, Yarden Y, Sela M. Persistent elimination of ErbB-2/HER2-overexpressing tumors using combinations of monoclonal antibodies: relevance of receptor endocytosis. Proc Natl Acad Sci U S A 2009;106(9):3294–9.
[31] Spangler JB, Neil JR, Abramovitch S, Yarden Y, White FM, Lauffenburger DA, et al. Combination antibody treatment down-regulates epidermal growth factor receptor by inhibiting endosomal recycling. Proc Natl Acad Sci U S A 2010;107(30): 13252–7.
[32] Toth G, Szoor A, Simon L, Yarden Y, Szollosi J, Vereb G. The combination of trastuzumab and pertuzumab administered at approved doses may delay development of trastuzumab resistance by additively enhancing antibody-dependent cell-mediated cytotoxicity. MAbs 2016;8(7):1361–70.
[33] Yamashita-Kashima Y, Iijima S, Yorozu K, Furugaki K, Kurasawa M, Ohta M, et al. Pertuzumab in combination with trastuzumab shows significantly enhanced antitumor activity in HER2-positive human gastric cancer xenograft models. Clin Cancer Res 2011;17(15):5060–70.
[34] Kamat V, Donaldson JM, Kari C, Quadros MR, Lelkes PI, Chaiken I, et al. Enhanced EGFR inhibition and distinct epitope recognition by EGFR antagonistic mAbs C225 and 425. Cancer Biol Ther 2008;7(5):726–33.
[35] Pedersen MW, Jacobsen HJ, Koefoed K, Hey A, Pyke C, Haurum JS, et al. Sym004: a novel synergistic anti-epidermal growth factor receptor antibody mixture with superior anticancer efficacy. Cancer Res 2010;70(2):588–97.
[36] Tvorogov D, Anisimov A, Zheng W, Leppanen VM, Tammela T, Laurinavicius S, et al. Effective suppression of vascular network formation by combination of antibodies blocking VEGFR ligand binding and receptor dimerization. Cancer Cell 2010;18(6):630–40.
[37] Ko BK, Lee SY, Lee YH, Hwang IS, Persson H, Rockberg J, et al. Combination of novel HER2-targeting antibody 1E11 with trastuzumab shows synergistic antitumor activity in HER2-positive gastric cancer. Mol Oncol 2015;9(2):398–408.
[38] Li X, Yang C, Wan H, Zhang G, Feng J, Zhang L, et al. Discovery and development of pyrotinib: a novel irreversible EGFR/HER2 dual tyrosine kinase inhibitor with favorable safety profiles for the treatment of breast cancer. Eur J Pharm Sci 2017;110:51–61.
[39] Spangler JB, Manzari MT, Rosalia EK, Chen TF, Wittrup KD. Triepitopic antibody fusions inhibit cetuximab-resistant BRAF and KRAS mutant tumors via EGFR signal repression. J Mol Biol 2012;422(4):532–44.